Peng-Robinson Equation of State Extended to Handle Aqueous Components Using CPA Concept

Henrik Sørensen[1,*], Rasmus Risum Boesen[1], Sukit Leekumjorn[2] and Peter Jørgensen Herslund[1]

[1]*Calsep A/S, Parallelvej 12, DK-2800 Kgs. Lyngby, DENMARK*
[2]*Calsep Inc., 10370 Richmond Avenue, Suite 1375, Tx 77042 Houston, USA*

Received December 22, 2017; Accepted March 06, 2018

Abstract: Parameters are presented enabling the Cubic Plus Association (CPA) concept to be applied with the Peng-Robinson equation for petroleum reservoir fluids carrying water and any of the gas hydrate inhibitors, methanol, mono-ethylene-glycol, or tri-ethylene-glycol. The acid gases, CO_2 and H_2S, are treated as solvating components, which do not self-associate, but cross-associate with water and hydrate inhibitors. Association is not considered for the remaining petroleum reservoir fluid constituents. The presented concept and parameters enable CPA to be used in flow assurance and process simulations on produced reservoir well streams containing water and hydrate inhibitors, while retaining consistency with prior reservoir simulations carried out using the Peng-Robinson equation on the water free reservoir fluid. A comprehensive data material for the mutual solubility of gases and aqueous components and hydrate inhibition is used to determine the pure component parameters and binary interaction parameters for associating components.

Keywords: CPA, Hydrate inhibitors, Peng-Robinson equation, Phase equilibrium, Water

1 Introduction

Water is usually treated as an inert phase in petroleum reservoir simulation studies. The impact of water on pressure, phase mobility, etc. is assessed, but mutual

**Corresponding author*: hs@calsep.com

DOI: 10.7569/JNGE.2018.692501

solubility with the components in the hydrocarbon phases is neglected. In flow assurance and process simulations, it is not in general acceptable to ignore the mutual solubility of aqueous and hydrocarbon phases. A reservoir fluid may for example be saturated with water from an underlying aquifer, in which case the solubility of water in the reservoir fluid at reservoir conditions will influence the amount of hydrate inhibitor required to avoid hydrate formation in a pipeline transporting the untreated well stream to a process plant.

Cubic equations of state are widely used in reservoir simulation studies. That is the case for compositional reservoir simulations as well as black oil simulations. A compositional reservoir simulator has its own built-in equation of state engine, while black oil simulators use look-up property tables generated using an equation of state (EoS) model. The EoS model parameters are tuned to match PVT data measured on the water free reservoir fluid. This so-called EoS model development can be quite time-consuming and it would be desirable if the EoS model developed could be reused in flow assurance and process simulations. In addition to a good representation of the water free reservoir fluid, pipeline and process simulations will usually require accurate simulation results for hydrate suppression and for the mutual solubility of water and hydrocarbon phases.

In their original forms, the cubic EoS-es are unsuited for mixtures with water and other aqueous components. The classical mixing rules are based on the assumption that the molecules in a phase are randomly distributed. This assumption is not fulfilled for mixtures containing water and other polar components. The molecules around a water molecule will have a higher concentration of water than the average water concentration in the phase. That can be accounted for by using a mixing rule based on a local composition excess Gibbs energy model as for example the Huron-Vidal mixing rule [1] or an association model combined with a cubic EoS. Kontogeorgis et al. [2] have successfully combined an association model based on the Wertheim theory [3] with the Soave-Redlich-Kwong (SRK) EoS [4]. Water and hydrate inhibitors as for example methanol (MeOH), mono-ethylene-glycol (MEG) and tri-ethylene-glycol (TEG) are examples of associating components. Molecules of an associating component may associate with molecules of the same chemical species (self-association) or with a molecule of a different chemical species (cross-association). The concept of combining a cubic EoS with an association model is called Cubic Plus Association (CPA) and is applicable to any cubic EoS, but most published work on the CPA concept is with SRK as underlying cubic EoS [5–11].

The volume corrected Peng-Robinson (PR) EoS [12–14] is one of the most commonly used cubic EoS-es in the oil industry. A large number of reservoir simulation studies are based on the PR EoS. If PR-CPA parameters were available for water and the most commonly used hydrate inhibitors, it would allow existing PR EoS parameter sets to be reused in flow assurance and process simulations considering those aqueous components. Since the PR-CPA EoS reduces to the classical PR EoS in the absence of associating components, a PR-CPA model would be fully

DOI: 10.7569/JNGE.2018.692501

consistent with a PR model developed for the water free reservoir fluid. To make use of the PR-CPA model, parameters are required for each self-associating and each cross-associating component. Binary interaction parameters for component pairs contained in the water free reservoir fluid can be reused, but an appropriate binary interaction parameter must be assigned to each component pair of at least one associating component.

The primary targets of the PR-CPA model in flow assurance and process simulations on produced well streams would be to simulate i) water content in gas, ii) loss of hydrate inhibitors to hydrocarbon phases, iii) gas hydrate inhibition. The key parameters to fulfill those targets are a correct representation of the pure associating components and of the interactions between associating components and between associating and non-associating components in gas and liquid phases. The association parameters and interaction parameters must be applicable at pressures and temperatures ranging from petroleum reservoir conditions to atmospheric conditions.

If compositional flow or process simulations are target areas, it is a further requirement that the model parameters do not introduce non-physical phase behavior in a reasonable temperature span outside the target temperature interval. Compositional flow or process simulators may use the temperature as iteration variable to converge the heat balance and the iteration scheme may include temperature estimates outside the temperature range covered by verified parameters.

2 Peng-Robinson Equation with Association Term

The CPA model concept exists in a number of variants. The PR-CPA modification used in this work is shown in Appendix A. The $\alpha(T)$ expression in Equation (A2) was used. The chosen model concept allows reuse of existing PR model parameter sets from reservoir simulation studies established on the basis of PVT data measured on a water free petroleum reservoir fluid composition. The hydrocarbons are assumed not to associate and their contribution to the EoS parameters are derived from critical pressure, temperature, and acentric factor in the same way as for the classical PR EoS. Water and the hydrate inhibitors, MeOH, MEG and TEG are components, which may associate with molecules of the same chemical species and molecules of other associating components. For those components, the critical properties are inapplicable to find EoS parameters for the CPA model.

To calculate the contribution from the cubic term of Equation (A1), appropriate binary interaction parameters must be determined for each pair of aqueous (associating) components and for pairs of one aqueous component and one petroleum reservoir fluid (non-associating) component. As expressed in Equation (A7), a linear dependence in temperature was used for the binary interaction parameters. It might have been possible to get a better match of the gas solubility in aqueous phases by using a second order temperature dependence, but that could possibly

DOI: 10.7569/JNGE.2018.692501

introduce unphysical phase behavior at very low and very high temperatures. The latter might prevent generation of complete phase diagrams for a reservoir fluid with water and a hydrate inhibitor and a physically meaningful solution to a flash calculation at very low and very high temperatures. The latter could present problems for a compositional flow simulator using the temperature as iteration variable during which iterations very low and very high temperatures can occur. For pairs of non-associating components, the binary interaction parameters from existing EoS models are reused.

Two modifications of the PR EoS are in common use in the oil industry, the original one from 1976 [12] and a modified one from 1978 [13]. They only differ for the m-parameter of components with high acentric factors (Equations (A3) and (A4)), and PR-CPA EoS parameters determined for associating components are applicable for both PR-modifications.

3 Existing PR-CPA Parameter Sets

The parameters entering into the volume corrected PR EoS are relatively well-defined as described in Appendix A. For each component, the parameters a_c and b are determined from the critical temperature (T_c) and critical pressure (P_c) to give an inflexion point on the PV isotherm at the critical point. Minor variations exist for the temperature term, $\alpha(T)$, which may be determined from an expression in acentric factor as proposed by Peng and Robinson [12, 13] (Equations (A2)–(A4)) or from an expression proposed by Mathias and Copeman [15] (Equations (A5)–(A6)).

The association term and how to determine association parameters for use with the CPA model concept are less standardized. The first choice is which underlying cubic EoS to use. The SRK and PR EoS-es are both commonly used in the oil industry. Although the two models are similar, the attractive term (a(T) in Equation (A1)) deviates and different parameters are needed to obtain the correct contributions from the non-associating and associating terms. CPA parameters determined for use with the SRK cubic EoS can therefore not be reused with PR as underlying cubic EoS.

The radial distribution function may be derived from Equation (A14) [5] as in this work, also referred to in literature as simplified CPA, or a more complicated expression [2] may be used. The cross-association parameters, $\varepsilon^{A_iB_j}$ and $\beta^{A_iB_j}$ in this work are determined using the CR-1 combining rules in Equations (A15) and (A16) [16], but could alternatively have been determined using combining rules proposed by Elliot [17]. For a classical cubic EoS, the parameters a and b are derived from the pure component critical temperatures, critical pressures, and acentric factors. In order to reuse existing EoS model parameters in simulations using the CPA concept for associating components, a and b parameters for non-associating components must still be derived that way. There are however examples in literature [8] that EoS parameters for non-associating

DOI: 10.7569/JNGE.2018.692501

components are determined differently to achieve better match of phase equilibrium data. The PR-CPA parameters for water, MeOH, MEG, and TEG in this work are determined with a volume correction of zero (c=0 in Equation (A1)), but a volume correction could have been applied also for associating components.

Five pure component parameters (a_0, b, c_1, ε^{AB}, and β^{AB}) must be determined for each associating component. They are usually determined to match the pure component vapor pressure and the density of saturated liquid. There will however be multiple parameter sets providing approximately the same match of those two properties. When the CPA concept is used, the molecular attractions are being distributed on two terms of the equation, the attractive part of the cubic term and the association term. Matching pure component vapor pressures and densities of saturated liquid only requires that the sum of these two contributions is correct, whereas interactions (mutual solubility) with other components requires that the split between the two terms is correct. Hence, binary data is needed to single out the pure component parameters providing a correct pure component behavior as well as a correct mutual solubility with other components. The binary data used will influence the pure component parameters and so will the relative importance given to solubility of associating (aqueous) components in non-aqueous phases and the solubility of non-aqueous components in the aqueous phase.

Binary interaction parameters enter as a corrective term in the mixing rule for the molecular attraction parameter, a, in the cubic term. The optimum interaction parameters for binaries with at least one associating component will depend on the binary data used when estimating pure component CPA parameters. For reasons outlined above, this work uses binary interaction parameters that are linear in temperature. Other functional forms, including a constant interaction parameter or a second order temperature dependence, could have been chosen. Table 1 summarizes the PR-CPA model concept used in this work and possible alternatives. It will only be possible to reuse PR-CPA parameters from literature, when the same model concept is used.

Wu and Prausnitz [18] have presented a PR-CPA parameter set for water. They use a different expression for the radial distribution function than Equation (A14) and constant binary interaction parameters. Water is assumed to have only three association sites and not four as in this work and most other CPA literature sources.

Li and Firoozabadi [19] have also presented PR-CPA parameters for water. They use the Matias-Copeman expression [15] for $\alpha(T)$ of water. In mixtures with CO_2, water is assigned a non-zero volume correction. Solvation is considered between water and the light hydrocarbons.

Hajiw et al [20] have estimated a PR-CPA pure component parameter set for water with emphasis on matching the gas solubility in the water phase by regressing binary interaction parameters. They use a group contribution method to generate binary interaction parameters, which are non-linear in temperature.

DOI: 10.7569/JNGE.2018.692501

Table 1 CPA model configuration used in this work and possible alternatives.

CPA parameter	This work	Alternatives
Cubic EoS	Peng-Robinson	Any cubic EoS. Most publications are about SRK [e.g. 5–11].
Pure component CPA parameters	Vapor pressure, saturated liquid density, and mutual solubility. For water and MeOH mutual solubility with methane was used weighting aqueous concentration in C_1 higher than C_1 concentration in aqueous phase. For MEG and TEG mutual solubility with nC_7 was used.	Vapor pressure, saturated liquid density, and mutual solubility with non-aqueous component. More weight may be on non-aqueous in aqueous or on aqueous in non-aqueous.
Radial distribution function	Equation (A14) also referred to in literature as simplified CPA [5]	More complicated expression [2]
Combining rules for two associating components	CR-1 [16]	Elliot [17]
Association scheme for H_2O	4C (two positive and two negative sites)	3B (3 sites) [18] and 2B (2 sites) [51]
Association scheme for MeOH	2B (one positive and one negative site)	–
Association scheme for MEG and TEG	4C (two positive and two negative sites)	–
Solvating components with water and hydrate inhibitors	CO_2 and H_2S	Hydrocarbon gas components in addition to CO_2 and H_2S [19]
$\alpha(T)$ for associating components	Functional form of Equation (A2)	Matias-Copeman expression [15]
EoS parameters a(T) and b of non-associating components	From classical cubic EoS	Tuning parameters [8]
Binary interaction parameter in cubic term	Linear in temperature	Constant [18], second order polynomial in temperature [21], or group contribution concept with non-linear temperature dependence [20]
Volume correction for associating components	Volume correction = 0	Volume correction ≠ 0 [19]

DOI: 10.7569/JNGE.2018.692501

Wang et al. [21] have presented pure component parameters set for water in a PR-CPA model with focus on modeling aqueous alkanol amine systems. They use a second order temperature dependence for the binary interaction parameters.

Having evaluated the published PR-CPA parameter sets, the conclusion was that none of them would fulfill the target of this work. New pure component PR-CPA parameters must be estimated to meet the target of this work.

4 Data Material and Estimation of PR-CPA Parameters

In order to apply the PR-CPA model concept on petroleum reservoir fluids with any of the components, water, MeOH, MEG, and TEG, five pure component parameters (a_0, b, c_1, ε^{AB}, and β^{AB}) must be determined for each of the four mentioned aqueous components. Those parameters were determined to match the pure component vapor pressure and densities of saturated liquid [22] while at the same time considering the mutual solubility with methane or nC_7. The references to the latter data are given in Tables 2–5. These tables also give references to the data used to determine interaction parameters for binaries with one or two associating components. Also shown are pressure and temperature ranges covered by experimental data for each component pair. The need for considering data for mutual solubility during determination of the pure component parameters is that multiple pure component parameter sets can give approximately the same match of pure component vapor pressure and densities of saturated liquid. The data for mutual solubility is used to single out the pure component parameter set providing the best match of both pure component vapor pressure and densities of saturated liquid and mutual solubility.

Association schemes expressed as number of negative charge sites (No. of ÷charge sites) and number of positive charge sites (No. of +charge sites) and the obtained pure component PR-CPA parameters for the associating components are shown in Table 6. The association schemes are illustrated graphically in Figure A1 in Appendix A.

A linear temperature dependence is used for the binary interaction parameters for pairs of associating components and for pairs of one associating component and one non-associating component. For pairs of water and another aqueous component, the interaction parameters are shown in Table 7. For MeOH and MEG, the interaction parameters were determined to match hydrate formation data for methane and for TEG hydrate formation data for methane and ethane. Binary interaction parameters of zero are used for other pairs of aqueous components.

CO_2 and H_2S are solvating components. They do not self-associate, but cross-associate with aqueous components. Cross-association volumes and interaction parameters were determined for CO_2 and each of the four aqueous components using the data in Tables 2–5. The data material for H_2S only allowed for cross-association volumes and interaction parameters to be determined for H_2O and MeOH as the aqueous component, hence for MEG and TEG as aqueous component

DOI: 10.7569/JNGE.2018.692501

DOI: 10.7569/JNGE.2018.692501

Table 2 Data material for mutual solubility of binary mixtures with water as the associating component.

Water (1)	Component (1) in component (2)					Component (2) in component (1)				
Component (2)	T_{min} [°C]	T_{max} [°C]	P_{min} [bar]	P_{max} [bar]	References	T_{min} [°C]	T_{max} [°C]	P_{min} [bar]	P_{max} [bar]	References
N_2	25.0	240.0	13.8	1349.0	[52–54]	1.1	240.0	4.3	1013.2	[23, 24, 55]
CO_2	0.2	205.2	1.0	3500.0	[56–60]	0.0	260.0	0.5	3500.0	[56, 58, 60, 61]
H_2S	25.0	204.4	3.4	353.1	[62–64]	10.0	204.4	1.5	206.9	[62–64]
C_1	0.0	250.0	5.1	1378.2	[11, 30–32, 40, 65–67, 68]	1.2	280.0	0.1	2583.1	[32–36, 40, 68, 69–71]
C_2	4.9	250.0	3.2	2910.0	[72, 73]	1.1	300.0	0.7	3500.0	[73, 74]
C_3	37.8	320.0	5.4	2000.0	[75, 76]	0.0	148.9	0.1	192.2	[75–77]
nC_4	37.8	237.8	1.4	694.0	[78, 79]	25.0	237.8	1.0	1000.0	[78–80]
nC_5	5.5	204.4	1.0	137.9	[81–84]	25.1	204.4	0.7	137.9	[84]
C_6 (nC_6)	172.4	275.0	19.6	784.5	[85–87]	7.7	80.0	1.0	5.0	[87–89]

Table 3 Data material for mutual solubility of binary mixtures with methanol as the associating component.

Methanol (1)	**Component (1) in component (2)**					**Component (2) in component (1)**				
Component (2)	T_{min} **[°C]**	T_{max} **[°C]**	P_{min} **[bar]**	P_{max} **[bar]**	**References**	T_{min} **[°C]**	T_{max} **[°C]**	P_{min} **[bar]**	P_{max} **[bar]**	**References**
N_2	–45.6	100.0	1.0	986.9	[90–92]	–50.0	100.0	1.0	1062.9	[90–92]
CO_2	–45.0	200.0	1.5	164.1	[93–97]	–45.0	150.0	<0.1	162.0	[93–97]
H_2S	25.0	175.0	0.9	112.0	[98]	–25.0	175.0	0.2	112.0	[98,99]
C_1	–53.2	160.2	6.9	1113.0	[100–102]	–73.2	175.0	0.4	1066.0	[100–102]
C_2	–31.8	100.0	1.7	60.8	[103, 104]	15.0	100.0	0.5	133.3	[103–105]
C_3	–20.0	119.9	1.0	54.1	[92, 106, 107]	–50.0	119.9	0.3	54.1	[90, 106–107]
nC_4	–8.9	160.0	1.9	1400.0	[108,109]	–9.3	196.8	0.7	1400.0	[108,109]
nC_5	–1.1	149.5	1.0	1400.0	[109–111]	4.5	149.5	1.0	1400.0	[109–111]
nC_6	–7.0	64.8	0.3	1505.0	[113–116]	–2.6	75.0	0.2	1504.0	[112–116]

DOI: 10.7569/JNGE.2018.692501

Table 4 Data material for mutual solubility of binary mixtures with mono-ethylene-glycol (MEG) as the associating component.

MEG (1)	Component (1) in Component (2)					Component (2) in Component (1)				
Component (2)	T_{min} [°C]	T_{max} [°C]	P_{min} [bar]	P_{max}[bar]	References	T_{min} [°C]	T_{max} [°C]	P_{min} [bar]	P_{max} [bar]	References
N_2	20.0	64.9	11.3	124.3	[117]	50.0	125.0	15.7	396.0	[117,118]
CO_2	0.1	150.0	12.2	220.6	[117, 119, 120]	14.9	150.0	0.3	384.0	[119–123]
H_2S	30.0	80.0	0.9	16.3	[124]	–10.0	125.0	<0.1	67.5	[120, 124, 125]
C_1	5.0	65.0	14.8	200.0	[102, 117, 126]	10.1	150.0	0.9	400.6	[112, 126–128]
C_2	/	/	/	/	–	10.1	125.0	1.0	203.4	[128, 129]
C_3	/	/	/	/	–	25.0	125.0	0.8	202.9	[130]
nC_6	10.0	57.2	1.0	1.0	[131, 132]	10.0	57.2	1.0	1.0	[131, 132]
nC_7	42.8	78.7	1.0	1.0	[131]	42.8	78.7	1.0	1.0	[131]

DOI: 10.7569/JNGE.2018.692501

Table 5 Data material for mutual solubility of binary mixtures with tri-ethylene-glycol (TEG) as the associating component.

TEG (1)	**Component (1) in component (2)**					**Component (2) in component (1)**				
Component (2)	T_{min} **[°C]**	T_{max} **[°C]**	P_{min} **[bar]**	P_{max} **[bar]**	**References**	T_{min} **[°C]**	T_{max} **[°C]**	P_{min} **[bar]**	P_{max} **[bar]**	**References**
CO_2	40.0	60.0	27.6	154.3	[133, 134]	23.9	125.0	1.0	202.5	[135, 136]
H_2S	/	/	/	/	–	23.9	125.0	<0.1	65.4	[135]
C_1	10.0	43.6	16.1	87.0	[137]	0.0	125.0	1.1	202.0	[135, 138]
C_2	/	/	/	/	–	25.0	125.0	1.1	204.8	[135]
C_3	/	/	/	/	–	23.9	125.0	0.2	64.5	[135]
nC_6	/	/	/	/	–	199.9	199.9	1.3	17.8	[139]
nC_7	36.2	77.8	1.0	1.0	[131]	36.2	77.8	1.0	1.0	[131]

DOI: 10.7569/JNGE.2018.692501

Table 6 PR-CPA pure component parameters and association schemes for self-associating components.

	T_c [K]	a_0 [bar/l²/mol²]	b [l/mol]	c_1 [–]	ε^{AB} [bar l/mol]	β^{AB} [–]	No. of ÷charge sites	No. of +charge sites
Water	647.3	1.5782	$1.4788 \cdot 10^{-2}$	0.6736	161.23	$6.9662 \cdot 10^{-2}$	2	2
MeOH	512.6	5.3485	$3.2112 \cdot 10^{-2}$	0.4310	236.87	$1.3239 \cdot 10^{-2}$	1	1
MEG	720.0	12.378	$5.1671 \cdot 10^{-2}$	0.6744	194.89	$1.4587 \cdot 10^{-2}$	2	2
TEG	769.5	44.349	$1.3253 \cdot 10^{-1}$	1.1692	143.37	$1.8273 \cdot 10^{-2}$	2	2

Table 7 Temperature dependent binary interaction parameter ($k_{ij} = k_{ij}^{ref} + k_{ij}' \cdot (T - T_{ref})$, where $T_{ref} = 288.15$K) for pairs of water and another aqueous component.

	MeOH			MEG			TEG		
	k_{ij}^{ref} [–]	k_{ij}' [1/K]	References	k_{ij}^{ref} [–]	k_{ij}' [1/K]	References	k_{ij}^{ref} [–]	k_{ij}' [1/K]	References
H_2O	–0.14146	$-4.257 \cdot 10^{-4}$	[42, 140, 141]	–0.07857	0	[124–125]	–0.19606	$6.411 \cdot 10^{-4}$	[48, 142]

only interaction parameters were determined. Cross-association energy was not determined as a tuning parameter but calculated from the association energy of the aqueous component as per Equation (A17) in Appendix A. The association schemes expressed as number of negative charge sites (No. of ÷charge sites) and number of positive charge sites (No. of +charge sites) and the cross-association volumes may be seen from Table 8 and the interaction parameters from Table 9. The association schemes are illustrated graphically in Figure A1 in Appendix A.

For pairs of one associating (aqueous) component and one hydrocarbon gas component, the interaction parameters were determined to give the best possible match of the mutual solubility. If the solubility of the aqueous component in the gas and the gas solubility in the aqueous phase could not both be matched well, the solubility of the aqueous component in the gas was given more importance. The resulting binary interaction parameters are shown in Table 9. For MEG and TEG, the interaction parameters for C_{7+} are set equal to the interaction parameter determined for nC_7. For H_2O and MeOH, parameters for the interaction with nC_7 were not estimated, hence their interaction parameters with the C_{7+} components in Table 9 are based on the trend seen for the lighter hydrocarbon components.

When estimating the five pure component parameters (a_0, b, c_1, ε^{AB}, and β^{AB}) of each aqueous component from data from vapor pressure and density of saturated liquid of the aqueous component and data for mutual solubility with one non-aqueous component, the object function was based on relative deviations between simulated and experimental values. Considerations about proper weighting between match of vapor pressure and of density of saturated liquid were done for each aqueous component. When estimating the kij for each binary system of one aqueous component and one non-aqueous component from data for mutual solubility, the object function was based on relative deviations between simulated and

DOI: 10.7569/JNGE.2018.692501

Table 8 PR-CPA cross-association volume parameter and association schemes for solvating components.

β^{AiBj} [–]	H_2O	MeOH	MEG	TEG	No. of ÷charge sites	No. of +charge sites
CO_2	0.15182	0.08219	0.13157	0.25000	1	0
H_2S	0.22248	0.13088	/	/	1	0

Table 9 PR-CPA parameters used in expression for temperature dependent binary interaction parameter ($k_{ij} = k_{ij}^{ref} + k_{ij}' \cdot (T - T_{ref})$, where T_{ref} = 288.15K).

	H_2O		MeOH		MEG		TEG	
	k_{ij}^{ref} [–]	k_{ij}' [1/K]	k_{ij}^{ref} [–]	k_{ij}' [1/K]	k_{ij}^{ref} [–]	k_{ij}' [1/K]	k_{ij}^{ref} [–]	k_{ij}' [1/K]
N_2	–0.10540	$2.905 \cdot 10^{-3}$	0.05911	0.00	0.36000	$-9.000 \cdot 10^{-5}$	0.15000	0.00
CO_2	0.07574	$6.649 \cdot 10^{-4}$	0.08651	$4.666 \cdot 10^{-4}$	0.20804	$5.179 \cdot 10^{-4}$	0.15882	$8.137 \cdot 10^{-4}$
H_2S	0.14736	$-1.305 \cdot 10^{-4}$	0.06009	$-1.368 \cdot 10^{-4}$	0.02213	$-2.312 \cdot 10^{-4}$	–0.06500	0
C_1	0.03833	$1.588 \cdot 10^{-3}$	0.00315	$-5.738 \cdot 10^{-5}$	0.09151	0	0.06000	0
C_2	0.07594	$9.937 \cdot 10^{-4}$	0.03001	$1.641 \cdot 10^{-5}$	0.06000	0	0.03000	0
C_3	0.04286	$8.697 \cdot 10^{-4}$	0.03582	$3.272 \cdot 10^{-4}$	0.05000	0	0.03000	0
iC_4/nC_4	0.00298	$7.507 \cdot 10^{-4}$	0.01500	$1.150 \cdot 10^{-4}$	0.05000	0	0.03000	0
iC_5/nC_5	0.00350	0	0.01000	$3.600 \cdot 10^{-4}$	0.05000	0	0.03000	0
C_6	–0.02	0	0.00870	$1.390 \cdot 10^{-4}$	0.05000	0	0.03000	0
C_{7+}	0	0	0.01	0	0.04000	0	0.03000	0

experimental values. Considerations about proper weighting between the solubility of the aqueous component in the non-aqueous component and of the non-aqueous component in the aqueous component were done for each binary system. When estimating the kij for each binary system of H_2O and each of the components MeOH, MEG and TEG from hydrate temperatures from hydrate inhibition data, the object function was based on absolute deviations between simulated and experimental values.

5 SIMULATION RESULTS

Table 10 summarizes the match of data for pure component vapor pressure and density of saturated liquid for the aqueous components. A good match is seen with PR-CPA for all the components. The deviation for vapor pressure of TEG is a little higher than for the other properties due to very low absolute vapor pressures at the lower temperatures.

Table 11 summarizes the match of data for mutual solubility in binary systems of H_2O and a non-aqueous component. For solubility of non-aqueous components in H_2O, the average deviation is less than 28%. For solubility of H_2O in

DOI: 10.7569/JNGE.2018.692501

Table 10 Absolute relative deviations (ARD) for match of pure component data.

	T_{min} [°C]	T_{max} [°C]	ARD for vapor pressure [%]	ARD for density of saturated liquid [%]
H_2O	0	370	0.7	2.0
MeOH	–50	230	1.9	0.6
MEG	50	425	0.7	1.6
TEG	50	470	5.7	2.7

Table 11 Absolute relative deviations (ARD) for match of data for mutual solubility in binary systems of H_2O (Component 1) and a non-aqueous component (Component 2).

Component (1)	**H_2O**	
Component (2)	**ARD for (1) in (2) [%]**	**ARD for (2) in (1)[%]**
N_2	12	12
CO_2	8	13
H_2S	12	13
C_1	10	14
C_2	11	28
C_3	18	10
nC_4	28	21
nC_5	20	3
C_6	33	20
nC_7	/	/

the non-aqueous components, the average deviation is less than 33%. The higher deviations are seen for the heavier hydrocarbon components, which will be present in small concentrations in a typical hydrocarbon gas phase. Graphical representations of the match for selected isotherms for the system C_1-H_2O are shown in Figures 1 and 2 below.

Table 12 summarizes the match of hydrate temperatures from hydrate inhibition data. Generally the match is within 2 °C with the exception of MeOH concentrations higher than 50 wgt% for which the match is within 4 °C. Graphical representations for selected concentrations of inhibitors are shown in Figures 3, 4, 5 and 6 below.

DOI: 10.7569/JNGE.2018.692501

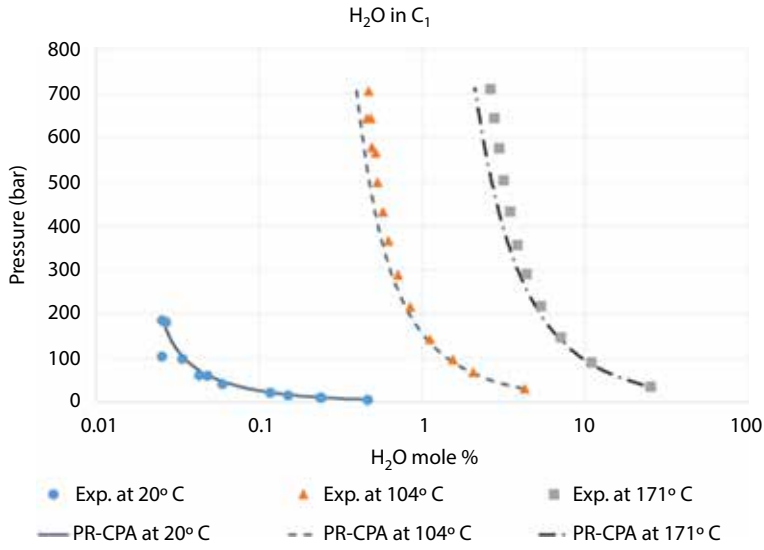

Figure 1 Water (H_2O) content in methane (C_1) at 20 °C, 104 °C and 171 °C and various pressures. Markers represent selected experimental data from [11,30–32]. Lines are model descriptions using PR-CPA.

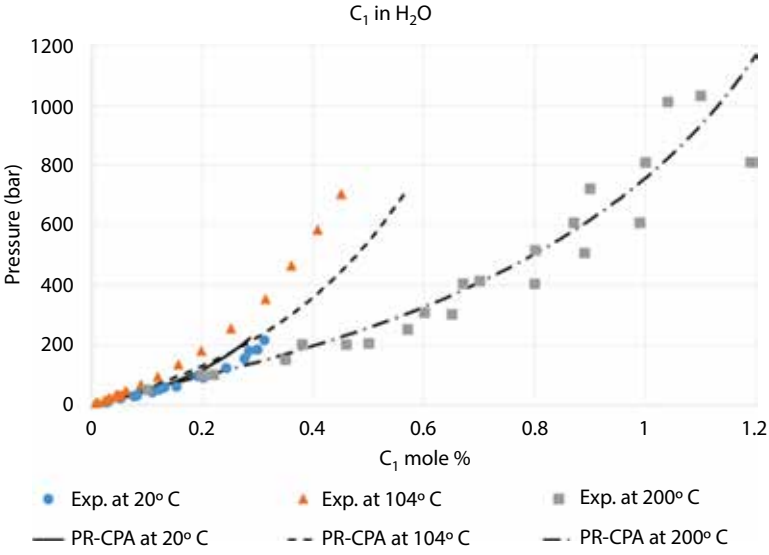

Figure 2 Solubility of methane (C_1) in water (H_2O) at 20 °C, 104 °C and 200°C and various pressures. Markers represent selected experimental data from [32–36]. Lines are model descriptions for PR-CPA.

DOI: 10.7569/JNGE.2018.692501

Table 12 Absolute deviations (AD) for match of hydrate temperatures from hydrate inhibition data.

	AD for hydrate temperature
MeOH	< 2 °C up to 50 wgt% inhibitor. < 4 °C above 50 wgt% inhibitor.
MEG	< 2 °C
TEG	< 2 °C

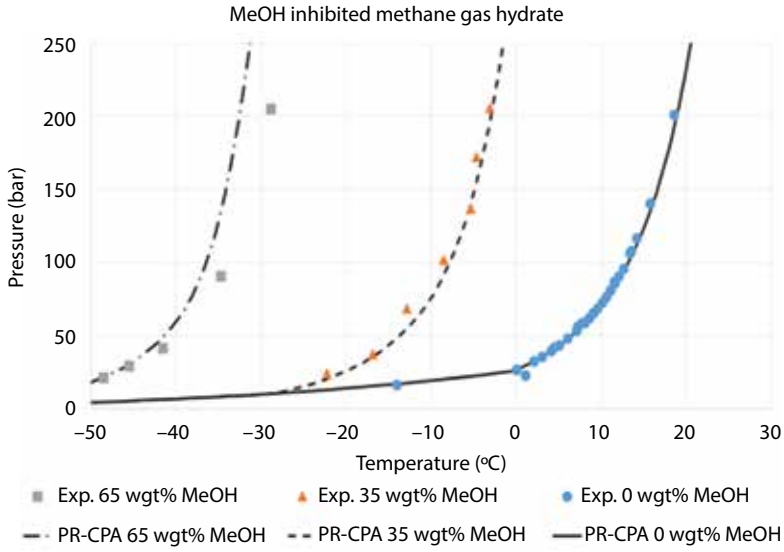

Figure 3 Methane hydrate formation conditions with various MeOH concentrations in the aqueous phase. Markers represent selected experimental data [42–45]. Lines are model descriptions for PR-CPA.

Figure 1 shows experimental data and simulation results for the water content in C_1 at three different temperatures ranging from 20 to 171 °C and pressures up to 700 bar. A very good match is seen with PR-CPA at all conditions.

Figure 2 shows experimental data and simulation results for the C_1 solubility in water at approximately the same temperatures and pressures as in Figure 1. Similar results as those shown in Figures 1 and 2 are obtained for other binary systems of one gas component and one aqueous component. The data at 200 °C appear as being internally inconsistent at the higher pressures. However, the data is mainly from three data sets each of which showing good consistency within the data set. Therefore, it is not obvious which data set should be excluded, hence all three data sets have been included.

DOI: 10.7569/JNGE.2018.692501

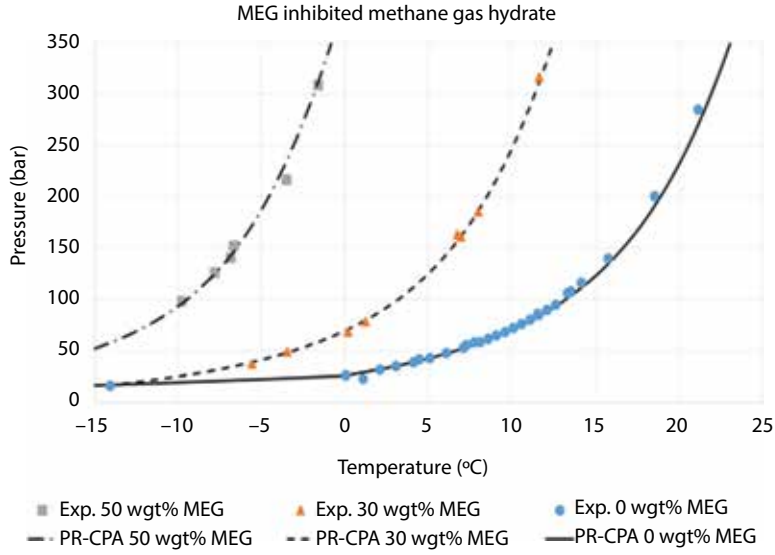

Figure 4 MEG hydrate formation conditions with various MEG concentrations in the aqueous phase. Markers represent selected experimental data [42–45, 46]. Lines are model descriptions for PR-CPA.

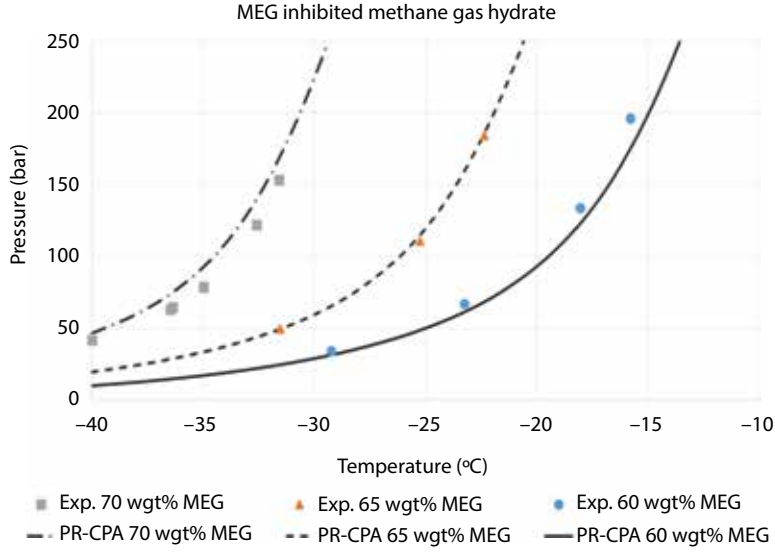

Figure 5 Mono-ethylene-glycol (MEG) inhibited methane gas hydrate at various weight (wgt) based concentrations of MEG in the aqueous phase. Markers represent selected experimental data from [47]. Lines are model descriptions for PR-CPA.

DOI: 10.7569/JNGE.2018.692501

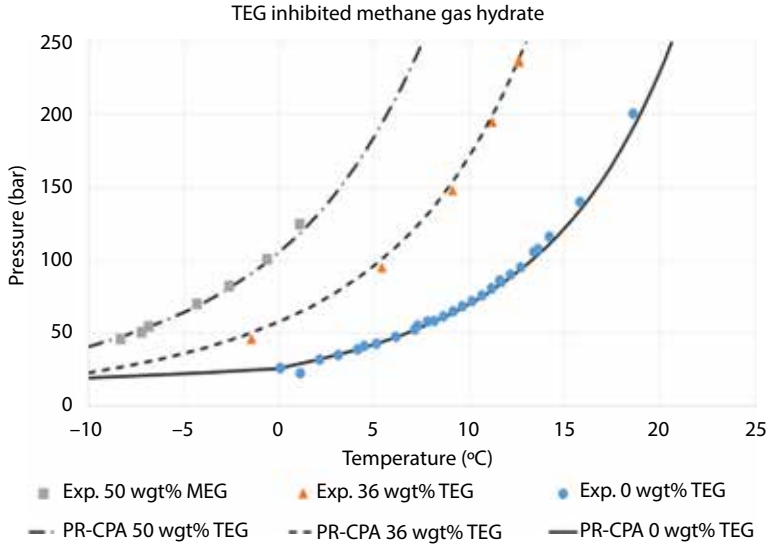

Figure 6 Tri-ethylene-glycol (TEG) inhibited methane gas hydrate at various weight (wgt) based concentrations of TEG in the aqueous phase. Markers represent selected experimental data [43–45, 48–50]. Lines are model descriptions for PR-CPA.

The water solubility in a CO_2 rich gas is particularly interesting as CO_2 is treated as a solvating component, which does not self-associate, but cross-associates with water. Figure 7 shows the water concentration in a gas consisting of 30 mole percent C_1 and 70 mole percent CO_2 at three different temperatures [23]. A good match is seen with PR-CPA.

The model parameters were determined from binary data and must be validated for multi-component systems. Figure 8 shows experimental data [24] and PR-CPA simulation results for the water content in a 4-component gas mixture with some content of the acid gases CO_2 and H_2S that are both modelled as solvating components. A very good match is seen between the data and the PR-CPA simulation results.

Table 13 shows a 7-component synthetic gas composition for which water solubility data and PR-CPA simulation results are shown in Figure 9. Some deviation is seen between the data point and the simulation result at the lowest pressure at 93 °C. The other data points are matched very well.

Figure 10 shows data and PR-CPA simulation results for the water content in a gas condensate at 1000 bar and temperatures ranging from 35 – 200 °C. The C_{7+} characterization procedure presented by Pedersen et al. [25] was applied for the reservoir fluid. The water concentration in the gas condensate phase is matched very well at 35 °C and 120 °C and reasonably well at 200 °C.

DOI: 10.7569/JNGE.2018.692501

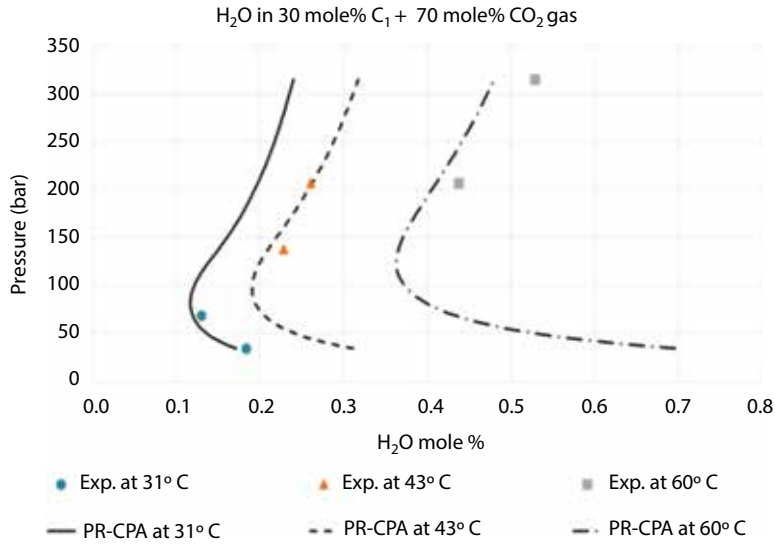

Figure 7 Water content in 30 mole% C_1 + 70 mole% CO_2 mixtures at 31°C, 43°C and 60°C and various pressures. Markers represent experimental data [37]. Lines are model predictions for PR-CPA.

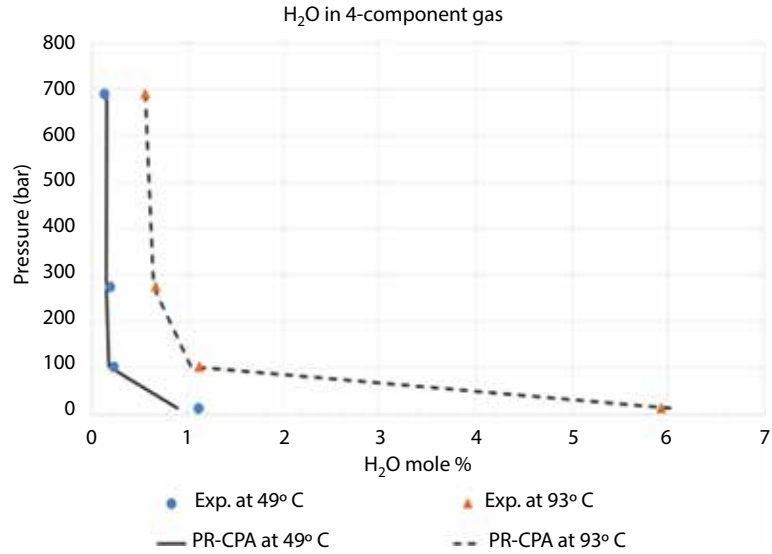

Figure 8 Water content in an acid gas mixture of 71.3 mole% C_1, 3.8 mole% C_3 18.8 mole% CO_2 and 6.3 mole% H_2S at 49°C and 93°C and various pressures. Markers represent experimental data [38]. Lines are model predictions for PR-CPA.

DOI: 10.7569/JNGE.2018.692501

Table 13 Synthetic gas composition for which data is shown in Figure 5.

Component	Mole%
C_1	67.5
C_2	4.5
C_3	1.9
iC_4	0.5
nC_4	0.7
CO_2	18.8
H_2S	6.3

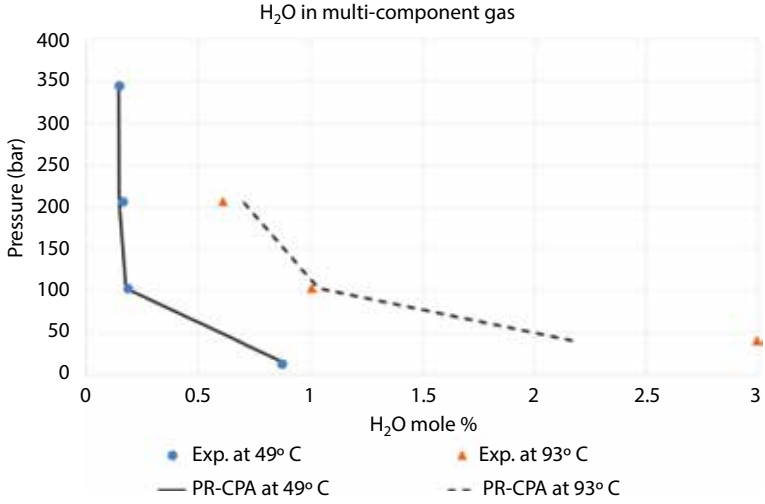

Figure 9 Water content in the synthetic gas mixture in Table 13 at 49°C and 93°C and various pressures. Markers represent experimental data [38]. Lines are model predictions for PR-CPA.

MeOH is one of the most commonly used hydrate inhibitors. The inhibition effect originates from the MeOH contained in the water phase. MeOH dissolved in the hydrocarbon phase has no hydrate suppression effect. If the water phase is small compared to the hydrocarbon phase(s), the percent MeOH loss to the hydrocarbon phase(s) can be considerable and must be taken into consideration when

DOI: 10.7569/JNGE.2018.692501

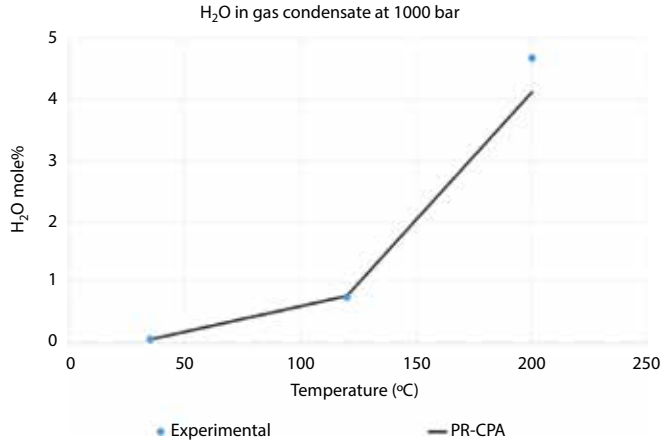

Figure 10 Water content in the gas condensate at 35–200 °C and a pressure of 1000 bar. Markers are experimental data [39]. Lines are model predictions for PR-CPA.

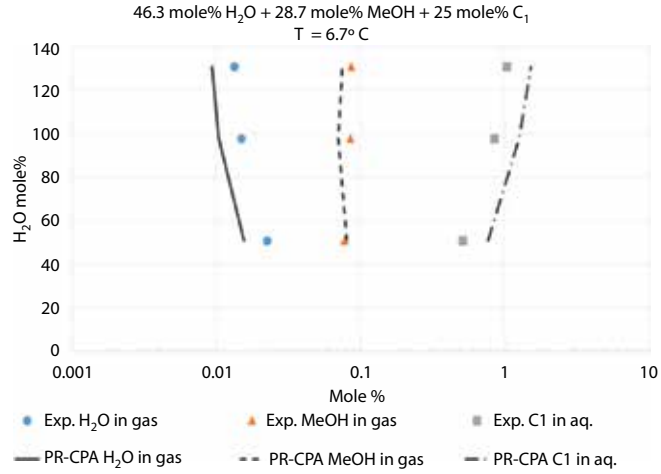

Figure 11 Compositional data for two-phase vapor-liquid equilibrium of the ternary system; water(H_2O)-methanol(MeOH)-methane(C_1) at 6.7°C. Markers represent experimental data [40]. Lines are model predictions for PR-CPA.

calculating the MeOH consumption needed to suppress the hydrate formation temperature sufficiently to avoid hydrate formation at relevant operating conditions. Such considerations are in principle also relevant for the two other hydrate inhibitors considered in this work, MEG and TEG, but they are much less volatile and less soluble in hydrocarbon phases than MeOH. Figure 11 shows experimental

DOI: 10.7569/JNGE.2018.692501

Table 14 Synthetic natural gas composition for which data is shown in Figures 12 and 13.

Component	Mole%
N_2	7.00
C_1	84.13
C_2	4.67
C_3	2.34
nC_4	0.93
nC_5	0.93

data and PR-CPA simulation results for the phase distribution in a 3-component mixture of H_2O, MeOH, and C_1. The simulation results provide a good match of the H_2O and MeOH concentrations in the gas phase as well as of the C_1 solubility in the aqueous phase.

While the loss of MEG to the hydrocarbon phases is limited, the water content in a hydrocarbon gas phase in equilibrium with a mixed H_2O-MEG phase is influenced by the MEG concentration. Table 14 shows a natural gas composition, which is contacted by an aqueous phase consisting of H_2O and MEG. Figure 12 shows data for the water content in the gas phase over an aqueous mixture with 50 weight percent MEG and Figure 13 data for the water content in the gas phase over an aqueous mixt ure with 70 weight percent MEG. PR-CPA simulation results for the water content in the gas phase are shown in both figures and match the experimental data closely.

A primary target of this work is to provide reliable PR-CPA model parameters for simulating fluid systems of a petroleum reservoir fluid, water, and a hydrate inhibitor. Pedersen et al. [26] have presented data for the MeOH partitioning between an aqueous, an oil and a vapor phase. The C_{7+} characterization procedure presented by Pedersen et al. [25] was applied for the reservoir fluid. The match of the data can be seen from Table 15.

MeOH, MEG and TEG may be added to reservoir fluid well streams carrying water to inhibit hydrate formation. The inhibitor concentration in the aqueous phase can be as high as 70 weight percent, and it is essential that the suppression of the hydrate temperature is simulated correctly in the whole concentration range. The hydrate model of Munck et al. [27] was used to test whether the PR-CPA model is capable of providing accurate simulation results for hydrate inhibition. Figure 3 shows hydrate formation data and PR-CPA simulation results for methane hydrate inhibited by MeOH up to a concentration of 65 weight percent. The simulation results agree well with the measured data.

DOI: 10.7569/JNGE.2018.692501

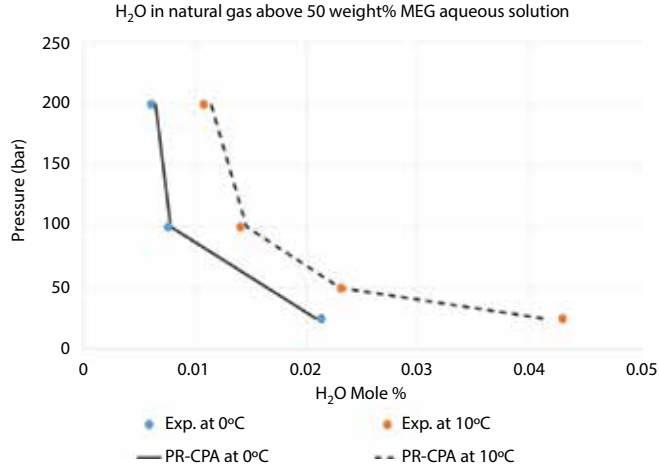

Figure 12 Water contents in gas phase at two-phase vapor-liquid equilibrium of the multi-component system; water(H_2O)-mono-ethylene glycol(MEG)-synthetic natural gas at 0 °C and 10 °C. Initial gas phase composition is given in Table 14. Initial aqueous phase is a 50 weight% MEG solution. Markers represent experimental data [41]. Lines are model predictions for PR-CPA.

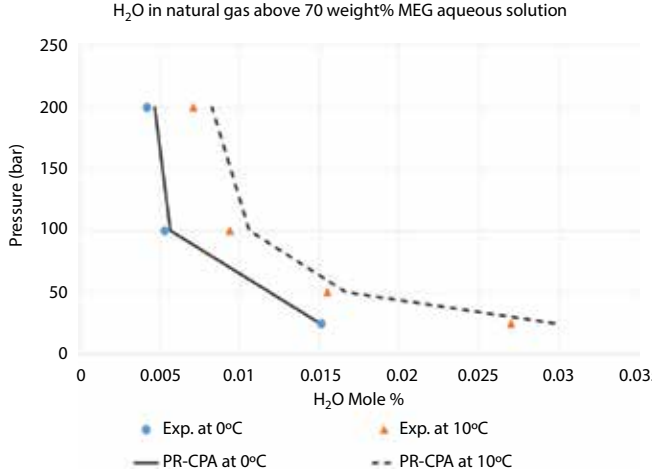

Figure 13 Water contents in gas phase at two-phase vapor-liquid equilibrium of the multi-component system; water(H_2O)-mono-ethylene glycol(MEG)-synthetic natural gas at 0 °C and 10 °C. Initial gas phase composition is given in Table 14. Initial aqueous phase is a 70 weight% MEG solution. Markers represent experimental data [41]. Lines are model predictions for PR-CPA.

DOI: 10.7569/JNGE.2018.692501

Table 15 Experimental data and simulation results for methanol distribution in a reservoir fluid. Reservoir fluid composition reported by Pedersen et al. [26]. RD is relative deviation in % of simulated phase composition compared to experimental phase composition.

		Exp. mole%	PR–CPA mole%	RD PR–CPA (%)
Aqueous phase	**Res. Fluid**	N/A	0.5673	N/A
	Methanol	18.6800	19.1744	2.65
	H_2O	81.3200	80.2584	–1.31
Oil phase	**Res. Fluid**	99.7990	99.8387	0.04
	Methanol	0.2010	0.1441	–28.28
	H_2O	N/A	0.0171	N/A
Vapor phase	**Res. Fluid**	99.9570	99.9506	–0.01
	Methanol	0.0429	0.0347	–19.20
	H_2O	N/A	0.0147	N/A

C_1 hydrate formation temperatures with MEG used as inhibitor in concentrations up to 50 weight percent is shown in Figure 4. Figure 5 shows C_1 hydrate formation temperatures for MEG concentrations up to 70 weight percent. In the whole concentration range, the PR-CPA simulations results agree well with the measured hydrate formation temperatures.

C_1 hydrate formation temperatures with TEG used as inhibitor in concentrations up to 50 weight percent is shown in Figure 6. In the whole concentration range, the PR-CPA simulations results agree well with the measured hydrate formation temperatures.

Conclusion

CPA association parameters capturing the pure component behavior for water, MeOH, MEG, and TEG have been determined for use with the Peng-Robinson equation of state. Binary interaction parameters linear in temperature have been determined for each pair of aqueous components and for each pair of an aqueous component and a gas component contained in a petroleum reservoir fluid (N_2, CO_2, H_2S, and hydrocarbon components). A comprehensive data material covering pressure and temperature conditions ranging from high pressure high temperature reservoir conditions to atmospheric conditions has been used. The data covers mutual solubility of aqueous (associating) components and gas components as well as hydrate formation data for systems with either MeOH, MEG or TEG used as inhibitor. CO_2 and H_2S are treated as solvating components, which do not self-associate, but cross-associate with aqueous components. Cross-association

DOI: 10.7569/JNGE.2018.692501

parameters are determined for those two components. The parameters allow existing PR models developed for water free reservoir fluids to be reused in PR-CPA simulations that are also to handle water and hydrate inhibitors. The presented parameters are applicable with the original PR equation of state from 1976 as well as the modification from 1978. The parameters have been validated against phase equilibrium data for multi-component systems and against hydrate data with varying inhibitor concentrations.

List of Notations

A	Association site
a	Parameter in Peng-Robinson equation of state
B	Association site
b	Parameter in Peng-Robinson equation of state
C_1-C_3	Constants in Mathias-Copeman expression (Equations (A5) and (A6)) for temperature dependence of a-parameter in a cubic equation of state.
CPA	Cubic Plus Association
CR-1	Cross-association combining rule
c	Volume correction
1.	EoS Equation of state
g	Radial distribution function
i	Component index
k_{ij}	Binary interaction parameter for i-j component pair
MEG	Mono-Ethylene-Glycol
MeOH	Methanol
m	Parameter defining temperature dependence of a
N	Number of components
NS	Number of association sites
P	Pressure
PR	Peng-Robinson
R	Gas constant
SRK	Soave-Redlich-Kwong
T	Temperature
TEG	Tri-Ethylene-Glycol
X	Fraction of non-bonded sites

Greek Letters

α	Parameter in Peng-Robinson equation of state
β	Association volume parameter
Δ	Association parameter defined in Equation (A13)
ε	Association energy parameter
η	Parameter is expression for radial distribution function defined in Equation (A14)
ω	Acentric factor

DOI: 10.7569/JNGE.2018.692501

Sub and Super indices

Association	Association term
0	Reference value
‘	Temperature derivative
Cubic	Cubic term
c	Critical property
i	Component index
j	Component index

References

1. M.J. Huron and J. Vidal, New mixing rules in simple equations of state for representing vapour-liquid equilibria of strongly non-ideal mixtures. *Fluid Phase Equilibria* **3**, 255–271 (1979).
2. G.M. Kontogeorgis, E.C. Voutsas, I.V. Yakoumis, and D.P. Tassios, An equation of state for associating fluids. *Ind. Eng. Chem. Res.* **35**(11), 4310–4318 (1996).
3. M. S. Wertheim, Fluids with highly directional attractive forces. I. Statistical Thermodynamics. II. Thermodynamic Perturbation Theory and Integral Equations. *Journal of Statistical Physics* **25**, 19–47 (1984).
4. G. Soave, Equilibrium constants from a modified Redlich-Kwong equation of state. *Chem. Eng. Sci.* **27**, 1197–1203 (1972).
5. G.M. Kontogeorgis, I.V. Yakoumis, H. Meijer, E. Hendriks, and T. Moorwood, Multicomponent Phase Equilibrium Calculations for Water–Methanol–Alkane Mixtures. *Fluid Phase Equilibria* **158**, 201–209 (1999).
6. G.K. Folas, G.M. Kontogeorgis, M.L. Michelsen and E.H. Stenby, Application of the cubic-plus-association equation of state to mixtures with polar chemicals and high pressures. *Ind. Eng. Chem. Res.* **45**(4), 1516–1526, (2006).
7. I. Tsivintzelis, G.M. Kontogeorgis, M.L. Michelsen, and E.H. Stenby, Modeling phase equilibria for acid gas mixtures using the CPA equation of state. Part II: Binary mixtures with CO2. *Fluid Phase Equilibria* **306**(1), 38–56 (2011).
8. I.V. Yakoumis, G.M Kontogeorgis, E.C. Voutsas, E.M. Hendriks, and D.P. Tassios, Prediction of phase equilibria in binary aqueous systems containing alkanes, cycloalkanes and alkenes with the cubic-plus-association equation of state. *Ind. Eng. Chem. Res.* **37**, 4175–4182 (1998).
9. G.M. Kontogeorgis, M.L. Michelsen, G.K. Folas, S. Derawi, N. von Solms, and E.H. Stenby, Ten years with the CPA (Cubic-Plus-Association) equation of state. Part 1. Pure compounds and self-associating systems. *Ind. Eng. Chem. Res.* **45**, 4855–4868 (2006).
10. S.O. Derawi, M.L. Michelsen, G.M. Kontogeorgis, and E.H. Stenby, Application of the CPA equation of state to glycol/hydrocarbons liquid-liquid equilibria. *Fluid Phase Equilibria* **209**, 163–184 (2003).
11. G.K. Folas, E.W. Froyna, J. Lovland, G.M. Kontogeorgis, and Even Solbraa, Data and prediction of water content of high pressure nitrogen, methane and natural gas. *Fluid Phase Equilibria* **252**(1–2), 162–174 (2007).
12. D.-Y. Peng and D.B. Robinson, A new two-constant equation of state. *Ind. Eng. Chem. Fundam.* **15**, 59–64 (1976).

DOI: 10.7569/JNGE.2018.692501

13. D.-Y. Peng and D.B. Robinson, The characterization of the heptanes and heavier fractions for the GPA Peng-Robinson programs. *GPA Research Report* **RR–28** (1978).
14. A. Peneloux, E. Rauzy, and R. Fréze, A consistent correlation for Redlich-Kwong-Soave volumes. *Fluid Phase Equilibria* **8**, 7–23 (1982).
15. P.M. Mathias and T.W. Copeman, Extension of the Peng-Robinson equation of state to complex mixtures: Evaluation of the various forms of the local composition concept. *Fluid Phase Equilibria* **13**, 91–108 (1983).
16. E.C. Voutsas, I.V. Yakoumis, and D.P. Tassios, Prediction of phase equilibria in water/alcohol/alkane systems. *Fluid Phase Equilibria* **158**, 151–163 (1999).
17. J.R. Elliot, S.J. Suresh, and M.D. Donohue, A simple equation of state for non-spherical and associating molecules. *Ind. Eng. Chem. Res.* **29**, 1476–1485 (1990).
18. J. Wu and J.M. Prauznitz, Phase equilibria for systems containing hydrocarbons, water, and salt: An extended Peng-Robinson equation of state. *Ind. Eng. Chem. Res.* **37**, 1634–1643 (1998).
19. Z. Li and A. Firoozabadi, Cubic-plus-association equation of state for water-containing mixtures: Is "Cross Association" necessary? *AIChE J.* **55**(7), 1803–1813 (2009).
20. M. Hajiw, A. Chapoy, and C. Coquelet, Hydrocarbons-water phase equilibria using the CPA equation of state with a group contribution method. *Can. J. Chem. Eng.* **93**, 432–442 (2015).
21. T. Wang, E. El Ahmar, and C. Coquelet, Alkane solubilities in aqueous alkanolamine solutions with CPA EoS. *Fluid Phase Equilibria* **434**, 93–101 (2017).
22. T.E. Daubert and R.P. Danner, *Physical and Thermodynamic Properties of Pure Compounds: Data Compilation*, Hemisphere, New York (2001).
23. R. Wiebe, V.L. Gaddy, and C. Heins, The solubility of nitrogen in water at 50, 75 and 100 degrees C from 25 to 1000 atmospheres. *J. Am. Chem. Soc.* **55**, 947–953 (1933).
24. A. Chapoy, A.H. Mohammadi, B. Tohidi, and D. Richon, Gas solubility measurement and modeling for the nitrogen + water system from 274.18 K to 363.02 K. *J. Chem. Eng. Data*, **49**(4), 1110–1115 (2004).
25. K.S. Pedersen, A.L. Blilie, and K.K. Meisingset, PVT calculations on petroleum reservoir fluids using measured and estimated compositional data for the plus fraction. *Ind. Eng. Chem. Res.* **31**(5), 1378–1384 (1992).
26. K.S. Pedersen, M.L. Michelsen, and A.O. Fredheim. Phase equilibrium calculations for unprocessed well streams containing hydrate inhibitors. *Fluid Phase Equilibria* **126**, 13–28 (1996).
27. J. Munck, S. Skjold-Jørgensen, and P. Rasmussen, Computations of the formation of gas hydrates. *Chem. Eng. Sci.* **43**(10), 2661–2672 (1988).
28. M.L. Michelsen and E.M. Hendriks, Physical properties from association models. *Fluid Phase Equilibria* **180**(1), 165–174 (2001).
29. A. Austegard, E. Solbraa, G. De Koeijer, and M.J. Mølnvik, Thermodynamic models for calculating mutual solubilities in H2O–CO2–CH4 Mixtures. *Chem. Eng. Res. Des.* **84**(9), 781–794 (2006).
30. R.H. Olds, B.H. Sage, and W.N. Lacey, Phase equilibria in hydrocarbon systems. Composition of the dew-point gas of the methane-water system. *Ind. Eng. Chem.* **34**(10), 1223–1227 (1942).
31. A.H. Mohammadi, A. Chapoy, D. Richon, and B. Tohidi, Experimental measurement and thermodynamic modeling of water content in methane and ethane systems. *Ind. Eng. Chem. Res.* **43**(22), 7148–7162 (2004).

DOI: 10.7569/JNGE.2018.692501

32. A. Chapoy, C. Coquelet, and D. Richon, Solubility measurement and modeling of water in the gas phase of the methane/water binary system at temperatures from 283.08 to 318.12 K and pressures up to 34.5 MPa. *Fluid Phase Equilibria* **214**, 101–117 (2003).
33. R.G. Sultanov, V.G. Skripka, and A.Y. Namiot, The solubility of methane in water at high temperatures and pressures. *Gazov. Prom.* **17**, 6–7 (1972).
34. Y. Wang, B. Han, H. Yan, and R. Liu, Solubility of CH4 in the mixed solvent t-butyl alcohol and water. *Thermochimica Acta* **253**, 327–334 (1995).
35. O.L. Culberson and J.J. Jr. McKetta, The solubility of methane in water at pressures to 10.000 PSIA. *Petrol. Trans. AIME* **192**, 223–226 (1951).
36. M. Yarrison, K.Y. Song, K.R. Cox, D. Chronister, and W. Chapman, Water content of high pressure, high temperature methane, ethane and methane + co2, ethane + CO2. *GPA Midstream Association GPA* **RR-200** (2008).
37. H.-J. Ng, C.-J. Chen, and H. Schroeder, Water content of natural gas systems containing acid gas. *GPA Midstream Association GPA* **RR-174**. (2001).
38. K.S. Pedersen, J. Milter, and C.P. Rasmussen, Mutual solubility of water and a reservoir fluid at high temperatures and pressures. experimental and simulated data. *Fluid Phase Equilibria* **189**, 85–97 (2001).
39. J.E. Davis and J.J. Jr. McKetta, Solubility of methane in water. *Petroleum Refiner*, **39**(3), 205–205 (1960).
40. M. Frost, E. Karakatsani, N. von Solms, D. Richon, and G.M. Kontogeorgis, Vapor-liquid equilibrium of methane with water and methanol. Measurements and modeling. *J. Chem. Eng. Data* **59**(4), 961–967 (2014).
41. A. Chapoy, R. Burgass, and B. Tohidi, Equilibrium water content in natural gas with hydrates or MEG solutions. *GPA Midstream Association GPA* **RR-211** (2011).
42. D.B. Robinson and H.-J. Chen, Hydrate formation and inhibition in gas condensate streams. *J. Can. Petrol. Technol.* **25**(4), 26–30 (1986).
43. T. Nakamura, T. Makino, T. Sugahara, and K. Ohgaki, Stability boundaries of gas hydrates helped by methane-structure-h hydrates of methylcyclohexane and cis-1,2-dimethylcyclohexane. *J. Chem. Eng. Sci.* **58**(2), 269–273 (2003).
44. O.L. Roberts, E.R. Brownscombe, and L.S. Howe, Constitution diagrams and composition of methane and ethane hydrates. *Oil Gas J.* **39**, 37–43 (1940).
45. J. Jhaveri and D.B. Robinson, Hydrates in the methane-nitrogen system. *Can. J. Chem. Eng.* **43**(2), 75–78 (1965).
46. H. Haghighi, A. Chapoy, R. Burgess, and B. Tohidi, Experimental and thermodynamic modelling of systems containing water and ethylene glycol: Application to flow assurance and gas processing. *Fluid Phase Equilibria* **276**(1), 24–30 (2009).
47. A. Chapoy and B. Tohidi, Hydrates in high inhibitor concentration systems. *GPA Midstream Association GPA* **RR-205** (2010).
48. A.H. Mohammadi and D. Richon, Gas hydrate phase equilibrium in methane + ethylene glycol, diethylene glycol, or triethylene glycol + water system. *J. Chem. Eng. Data* **56**(12), 4544–4548 (2011).
49. Rock, A. *Fortschritts-ber. VDI* **Reihe 3**, 1–279 (2003).
50. W. Afzal, A.H. Mohammadi, and D. Richon, Experimental measurements and predictions of dissociation conditions for carbon dioxide and methane hydrates in the presence of triethylene glycol aqueous solutions. *J. Chem. Eng. Data* **52**(5), 2025–2055 (2007).

DOI: 10.7569/JNGE.2018.692501

51. A. T. Zoghi, F. Feyzi, and M.R. Dehghani, Modeling CO_2 solubility in Aqueous *N*-methyldiethanolamine solution by electrolyte modified Peng–Robinson plus association equation of state. *Ind. Eng. Chem. Res.* **51**(29), 9875–9885 (2012).
52. V.V. Ugrozov, Equilibrium compositions of vapor-gas mixtures over solutions. *Russ. J. Phys. Chem.* **70**(7), 1240–1241 (1996).
53. V.Y. Maslennikova, N.A. Vdovina, and D.S. Tsiklis, Solubility of water in compressed nitrogen. *Russ. J. Phys. Chem.* **45**(9), 1354–1354 (1971).
54. A.H. Mohammadi, A. Chapoy, B. Tohidi, and D. Richon, Water content measurement and modeling in the nitrogen + water system. *J. Chem. Eng. Data* **50**(2), 541–545 (2005).
55. A.W. Saddington and N.W. Krase, Vapor-liquid equilibria in the system nitrogen-water. *J. Am. Chem. Soc.* **56**(2), 353–361 (1934).
56. K. Toedheide and E.U. Franck, Two-phase range and the critical curve in the system carbon dioxide-water up to 3500 bar. *Z. Phys. Chem. (München)* **37(5–6)**. 387–401 (1963).
57. I.P. Sidorov, Y.S. Kazarnovskii, and A.M. Goldman, The solubility of water in compressed gases. *Tr. Gos. NIPI Azot. Prom.* **1**, 48–67 (1953).
58. A. Bamberger, G. Sieder, and G. Maurer, High-pressure (Vapor-Liquid) equilibrium in binary mixtures of (Carbon Dioxide + Water or Acetic Acid) at temperatures from 313 to 353 K. *J. Supercrit. Fluids* **17**, 97–110 (2000).
59. F. Tabasinejad, R.G. Moore, S.A. Mehta, K.C. van Fraassen, Y. Barzin, J.A. Rushing, and K.E. Newsham, Water solubility in supercritical methane, nitrogen, and carbon dioxide: Measurement and modeling from 422 to 483 K and pressures from 3.6 to 134 MPa. *Ind. Eng. Chem. Res.* **50**(7), 4029–4041 (2011).
60. S.-X. Hou, G.C. Maitland, and J.P.M Trusler, Measurement and modeling of the phase behavior of the (Carbon Dioxide + Water) mixture at temperatures from 298.15K to 448.15K. *J. Supercrit. Fluids* **73**, 87–96 (2013).
61. P.B. Stewart and P. Munjal, Solubility of carbon dioxide in pure water, synthetic sea water, and synthetic sea water concentrates at -5 deg. to 25 deg. and 10 to 45 atm. pressure. *J. Chem. Eng. Data* **15**(1), 67–71 (1970).
62. F.T. Selleck, L.T. Carmichael, and B.H. Sage, Phase behavior in the hydrogen sulfide-water system. *Ind.Eng.Chem.* **44**(9), 2219–2226 (1952).
63. J.I. Lee and A.E. Mather, Solubility of hydrogen sulfide in water. *Ber. Bunsen-Ges. Phys. Chem.* **81**(10), 1020–1023 (1977).
64. A. Chapoy, H. Mohammadi, B. Tohidi, A. Valtz, and D. Richon, Experimental measurement and phase behavior modeling of hydrogen sulfide-water binary system. *Ind. Eng. Chem. Res.* **44**(19), 7567–7574 (2005).
65. M. Yarrison, K.R. Cox, and W.G. Chapman, Measurement and modeling of the solubility of water in supercritical methane and ethane from 310 to 477 K and pressures from 3.4 to 110 MPa. *Ind. Eng. Chem. Res.* **45**(20), 6770–6777 (2006).
66. A. Chapoy, H. Haghighi, R. Burgass, and B. Tohidi, Gas hydrates in low water content gases: Experimental measurements and modelling using the CPA equation of state. *Fluid Phase Equilibria* **296**(1), 9–14 (2010).
67. M. Sanchez and F. de Meer, Liquid-vapor equilibrium in the methanol-water system measured at high pressures and temperatures between 150 and 300°C. *Anal.Quim.* **74**, 1325–1328 (1978).
68. Y.-Q. Tian, Y.-L. Tian, L. Zhao, R.-J. Zhu, and C. Ma, Gas-liquid phase boundary lines and critical curve for the water + methane system. *Wuli-Huaxue-Xuebao* **28**(8), 1803–1808 (2012).

DOI: 10.7569/JNGE.2018.692501

69. J.J. Carroll, F.-Y. Jou, A.E. Mather, and F.D. Otto, The solubility of methane in aqueous solutions of monoethanolamine, diethanolamine and triethanolamine. *Can. J. Chem. Eng.* **76**, 945–951 (1998).
70. K. Lekvam and P.R. Bishnoi, Dissolution of methane in water at low temperatures and intermediate pressures. *Fluid Phase Equilibria* **131**, 297–309 (1997).
71. M. Yarrison, K.R. Cox, and W.G. Chapman, Measurement and modeling of the solubility of water in supercritical methane and ethane from 310 to 477 K and pressures from 3.4 to 110 MP. *Ind. Eng. Chem. Res.* **45**(20), 6770–6777 (2006).
72. L.-K. Wang, G.-J. Chen, G.-H. Han, X.-Q. Guo, and T.-M. Guo, Experimental study on the solubility of natural gas components in water with or without hydrate inhibitor. *Fluid Phase Equilibria* **207(1–2)**. 143–154 (2003).
73. A.H. Mohammadi A.H., A. Chapoy, B. Tohidi, and D. Richon, Measurements and thermodynamic modeling of vapor-liquid equilibria in ethane-water systems from 274.26 to 343.08 K. *Ind. Eng. Chem. Res.* **43**(17), 5418–5424 (2004),
74. A. Chapoy, C. Coquele, and D. Richon, Measurement of the water solubility in the gas phase of the ethane + water binary system near hydrate forming conditions. *J. Chem. Eng. Data* **48**(4), 957–966 (2003).
75. R. Kobayashi and D.L. Katz, Vapor-liquid equilibria for binary hydrocarbon-water systems. *Ind. Eng. Chem.* **45**(2), 440–451 (1953).
76. M. Sanchez and R. Coll, Propane-water system at high pressures and temperatures. I. Two-phase region. *Anal. Quim.* **74**, 1329–1335 (1978).
77. A. Chapoy, S. Mokraoui, A. Valtz, D. Richon, A.H. Mohammadi, and B. Tohidi, Solubility measurement and modeling for the system propane-water from 277.62 to 368.16 K. *Fluid Phase Equilibria* **226**, 213–220 (2004).
78. A. Danneil, K. Toedheide, and E.U. Franck, Vapor-liquid equilibria and critical curves of the systems ethane - water and n-butane - water at high pressures. *Chem. Ing. Tech.* **CIT**, **39**(13), 816–821 (1967).
79. H.H. Reamer, B.H. Sage, and W.N. Lacey, Phase equilibria in hydrocarbon systems. n-butane-water system in the two-phase region. *Ind. Eng. Chem.* **44**(3), 609–615 (1952).
80. J.J. Carroll, F.-Y, Jou, and A.E. Mather, Fluid phase equilibria in the system n-Butane + water. *Fluid Phase Equilibria* **140**, 157–169 (1997).
81. S.M. Rasulov and I.M. Abdulagatov, PVT measurements of water-n-pentane mixtures in critical and supercritical regions. *J. Chem. Eng. Data* **55**(9), 3247–3261 (2010).
82. C. Black, G.G. Joris, and H.S. Taylor, The solubility of water in hydrocarbons. *J. Chem. Phys.* **16**(5), 537–543 (1948).
83. S. Mokraoui, A. Valtz, C. Coquelet, and D. Richon, Mutual solubility of hydrocarbons and amines. *GPA Research Rep., Rep. No.* **RR–195**, 1–90 (2008).
84. P.C. Gillespie and G.M. Wilson, Vapor-liquid and liquid-liquid equilibria: Water-Methane; Water-Carbon Dioxide; Water-Hydrogen Sulfide; Water-nPentane; Water-Methane-nPentane. *GPA Research Rep., Rep.No.* **RR–48**, 1–73 (1982).
85. S.D. Burd and W.G. Braun, Vapor-liquid equilibrium of some c6 hydrocarbons with water. *Proc. Am. Petrol. Inst. Ref. Div.* **48**, 464–476 (1968).
86. R.G. Sultanov and V.G. Skripka, Solubility of water in n-alkanes at elevated temperatures and pressures. *Viniti* **Code 4386–72**, 1–13 (1972).
87. A.Y. Namiot, V.G. Skripka, and Y.G. Lotter, Phase equilibria in hydrocarbon - water systems at high temperatures. *Viniti* **Code 1213–76**, 1–13 (1976).

DOI: 10.7569/JNGE.2018.692501

88. A. Chapoy, H. Haghighi, and B. Tohidi, Development of a Henry's constant correlation and solubility measurements of n-pentane, i-pentane, cyclopentane, n-hexane, and toluene in water. *J. Chem. Thermodyn.* **40**(6), 1030–1037 (2008).
89. S. Mokraoui, C. Coquelet, A. Valtz, P.E. Hegel, and D. Richon, New solubility data of hydrocarbons in water and modeling concerning vapor-liquid-liquid binary systems. *Ind. Eng. Chem. Res.* **46**(26), 9257–9262 (2007).
90. W.-M., Melzer, Beitrag zur experimentellen Untersuchung von Gas-Flüssigkeits-Phasengleichgewichten, Thesis, TU Berlin (1990).
91. H. Lazalde-Crabtree, G.J.F. Breedveld, and J.M. Prausnitz, Solvent losses in gas absorption. Solubility of methanol in compressed natural and synthetic gases. *AIChE J.* **26**(3), 462–470 (1980).
92. T. Laursen and S.I. Andersen., High-pressure vapor–liquid equilibrium for nitrogen + methanol. *J. Chem. Eng. Data* **47**(5), 1173–1174 (2002).
93. E. Brunner, W. Hueltenschmidt, and G. Schlichthaerle, Fluid mixtures at high pressures IV. Isothermal phase equilibria in binary mixtures consisting of (Methanol + Hydrogen or Nitrogen or Methane or Carbon Monoxide or Carbon Dioxide). *J. Chem. Thermodyn.* **19**, 273–291 (1987).
94. J.H. Hong and R. Kobayashi, Vapor-liquid equilibrium studies for the carbon dioxide-methanol system. *Fluid Phase Equilibria* **41**, 269–276 (1988).
95. S.N. Joung, C.W. Yoo, H.Y. Shin, S.Y. Kim, K.-P Yoo, C.S. Lee, and W.S. Huh, Measurements and correlation of high-pressure VLE of binary CO2–alcohol systems (Methanol, Ethanol, 2-methoxyethanol and 2-ethoxyethanol). *Fluid Phase Equilibria* **185**, 219–230 (2001).
96. P. Naidoo, D. Ramjugernath, and J.D. Raal, A new high-pressure vapour–liquid equilibrium apparatus. *Fluid Phase Equilibria* **269(1–2)**. 104–112 (2008).
97. C. Secuianu, V. Feroiu, and D. Geana, Phase equilibria experiments and calculations for carbon dioxide + Methanol binary system. *Cent. Eur. J. Chem.* **7**(1), 1–7 (2009).
98. A.-D. Leu, J.J. Carroll, and D.B. Robinson, The equilibrium phase properties of the methanol-hydrogen sulfide binary system. *Fluid Phase Equilibria* **72**, 163–172 (1992).
99. M. Yorizane, S. Sadamoto, H. Masuoka, and Y. Eto, Gas solubilities in methanol at high pressure. *Kogyo Kagaku Zasshi* **72**, 2174–2177 (1969).
100. A.Z. Francesconi, Critical Curve, Phase Equilibria and PVT-Data of Methanol-Methane to 240°C and 3 kbar, Thesis, TH Karlsuhe (1978).
101. J.H. Hong, P.V. Malone, M.D. Jett, and R. Kobayashi, The measurement and interpretation of the fluid-phase equilibria of a normal fluid in a hydrogen bonding solvent: The methane-methanol system. *Fluid Phase Equilibria* **38**(1–2), 83–96 (1987).
102. M. Frost, Measurement and Modelling of Phase Equilibrium of Oil - Water - Polar Chemicals, Thesis, Technical University of Denmark (DTU), Lyngby (2014).
103. Y.H. Ma and J.P. Kohn, Multiphase and volumetric equilibria of the ethane-methanol system at temperatures between -40 °C. and 100 °C. *J. Chem. Eng. Data* **9**(1), 3–5 (1964).
104. L. Ruffine, Équilibres de Phases à Basse Température de Systèmes Complexes CO2 - Hydrocarbures Légers - Méthanol - Eau : Mesures et Modélisation, Thesis, Université Claude Bernard, Lyon (2005).
105. V. Roskar, R.A. Dombro, G.A. Prentice, C.R. Westgate, and M.A. McHugh, Comparison of the dielectric behavior of mixtures of methanol with carbon dioxide and ethane in the mixture-critical and liquid regions. *Fluid Phase Equilibra* **77**, 241–259 (1992).

DOI: 10.7569/JNGE.2018.692501

106. A.-D. Leu, D.B. Robinson, S.Y.-K. Chung, and C.-J. Chen, The equilibrium phase properties of the propane-methanol and n-butane-methanol binary systems. *Can. J. Chem. Eng.* **70**, 330–334 (1992).
107. S.N. Joung, H.Y. Shin, H.S. Kim, and K.-P. Yoo., High-pressure vapor–liquid equilibrium data and modeling of propane + methanol and propane + ethanol systems. *J. Chem. Eng. Data* **49**(3), 426–429 (2004).
108. X. Courtial, C.-B. Soo, C. Coquelet, P. Paricaud, D. Ramjugernath, and D. Richon, Vapor–liquid equilibrium in the n-butane + methanol system, measurement and modeling from 323.2 to 443.2 K. *Fluid Phase Equilibria* **277**(2), 152–161 (2009).
109. U. Haarhaus and G.M. Schneider, (Liquid + Liquid) phase equilibria in (Methanol + Butane) and (Methanol + Pentane) at pressures from 0.1 to 140 MPa. *J. Chem. Thermodyn.* **20**, 1121–1129 (1988).
110. F.G. Tenn and R.W. Missen, A study of the condensation of binary vapors of miscible liquids: Part I: The equilibrium relations. *Can. J. Chem. Eng.* **41**, 12–14 (1963).
111. R.A. Wilsak, S.W. Campbell, and G. Thodos, Vapor-liquid equilibrium measurements for the n-pentane-methanol System at 372.7, 397.7 and 422.6 K. *Fluid Phase Equilibria* **33(1–2)**. 157–171 (1987).
112. I.F. Hölscher, G.M. Schneider, and J.B. Ott, Liquid-liquid phase equilibria of binary mixtures of methanol with hexane, nonane and decane at pressures up to 150 MPA. *Fluid Phase Equilibria* **27**, 153–169 (1986).
113. H. Matsuda, K. Kurihara, K. Ochi, and K. Kojima, Prediction of liquid–liquid equilibria at high pressure for binary systems using EOS-GE models: Methanol + hydrocarbon. *Fluid Phase Equilibria* **203**, 269–284 (2002).
114. A. Iguchi, Vapor-liquid equilibrium at 25 °C for binary systems between alcohols and hydrocarbons. *Kagaku Sochi* **20**(3), 66–68 (1978).
115. A.M. Blanco and J. Ortega, Experimental study of miscibility, density and isobaric vapor-liquid equilibrium values for mixtures of methanol in hydrocarbons (C5, C6). *Fluid Phase Equilibria* **122**, 207–222 (1996).
116. A. Zawisza, High-Pressure liquid-vapour equilibria, critical state, and p(Vm, T, x) to 448.15 K and 4.053 MPa for {xC6H14 + (1−x)CH3OH}. *J. Chem. Thermodyn.* **17**, 941–947 (1985).
117. H. Schlichting, Experimentelle Bestimmung und Korrelierung der Löslichkeit verschiedener Lösungsmittel in Hochdruckgasen, Thesis, TU-Berlin (1991).
118. D.-Q. Zheng, W.-D. Ma, R. Wei, and T.-M. Guo, Solubility study of methane, carbon dioxide and nitrogen in ethylene glycol at elevated temperatures and pressures. *Fluid Phase Equilibria* **155**, 277–286 (1999).
119. Y. Adachi, P. Malone, T. Yonemoto, and R. Kobayashi, Glycol vaporization loss in super-critical CO2, *GPA Research Rep. Rep. No.* **RR–98**, 1–20 (1986).
120. F.-Y Jou, R.D. Deshmukh, F.D. Otto, and A.E. Mather, vapor-liquid equilibria of h2s and co2 and ethylene glycol at elevated pressures. *Chem. Eng. Commun.* **87**(1), 223–231 (1990).
121. D.-Q. Zheng, W.-D. Ma, R. Wei, and T.-M. Guo, Solubility study of methane, carbon dioxide and nitrogen in ethylene glycol at elevated temperatures and pressures. *Fluid Phase Equilibria* **155**, 277–286 (1999).
122. A.C. Galvao and A.Z. Francesconi, Solubility of methane and carbon dioxide in ethylene glycol at pressures up to 14 MPa and temperatures ranging from (303 to 423) K. *J. Chem. Thermodyn.* **42**(5), 684–688 (2010).

DOI: 10.7569/JNGE.2018.692501

123. F. S. Serpa, R.S. Vidal, J.H.B Amaral-Filho, J.F do Nascimento, J.R.P. Ciambelli, C.M.S. Figueiredo, G.R. Salazar-Banda, A.F. Santos, M. Fortuny, E. Franceschi, and C. Dariva, Solubility of carbon dioxide in ethane-1,2-diol–water mixtures. *J. Chem. Eng. Data* **58**(12), 3464–3469 (2013).
124. M. Shokouhi, A.R. Rezaierad, S.-M. Zekordi, M. Abbasghorbani, and M. Vahid, Solubility of hydrogen sulfide in ethanediol, 1,2-propanediol, 1-propanol, and 2-propanol: experimental measurement and modeling. *J. Chem. Eng. Data* **61**(1), 512–524 (2016).
125. I. Short I., A. Sahgal, and W. Hayduk, Solubility of ammonia and hydrogen sulfide in several polar solvents. *J. Chem. Eng. Data* **28**(1), 63–66 (1983).
126. G.K. Folas, O.J. Berg, E. Solbraa, A.O. Fredheim, G.M. Kontogeorgis, M.L. Michelsen, and E.H. Stenby, High-pressure vapor-liquid equilibria of systems containing ethylene glycol, water and methane - experimental measurements and modeling. *Fluid Phase Equilibria* **251**(1), 52–58 (2007).
127. F.-Y. Jou, F.D. Otto, and A.E. Mather, Solubility of methane in glycols at elevated pressures. *Can. J. Chem. Eng.* **72**, 130–133 (1994).
128. L.-K. Wang, G.-J. Chen, G.-H. Han, X.-Q. Guo, and T.-M., Guo, Experimental study on the solubility of natural gas components in water with or without hydrate inhibitor. *Fluid Phase Equilibria* **207(1–2)**. 143–154 (2003).
129. F.-Y. Jou, K.A.G. Schmidt, and A.E. Mather, Vapor–liquid equilibrium in the system ethane + ethylene glycol. *Fluid Phase Equilibria* **240**(2), 220–223 (2006).
130. F.-Y. Jou, F.D. Otto, and A.E. Mather, The solubility of propane in 1,2-ethanediol at elevated pressures. *J. Chem. Thermodyn.* **25**, 37–40 (1993).
131. S. O. Derawi, G.M. Kontogeorgis, E.H. Stenby, T. Haugum, and A.O. Fredheim, Liquid-liquid equilibria for glycols plus hydrocarbons: Data and correlation. *J. Chem. Eng. Data* **47**(2), 169–173 (2002).
132. A. Razzouk, R.A. Naccoul, I. Mokbel, P. Duchet-Suchaux, J. Jose, E. Rauzy, and C. Berro, Liquid–liquid equilibria for monoethylene glycol + hexane and 2,2,4-trimethylpentane, water + hexane and 2,2,4-trimethylpentane, monoethylene glycol + water + hexane, and monoethylene glycol + water + 2,2,4-trimethylpentane in the temperature range between T= 283.15 K and T= 323.15 K. *J. Chem. Eng. Data* **55**(4), 1468–1472 (2010).
133. G.-I. Kaminishi, S. Takano, C. Yokoyama, and S. Takahashi, Concentration of triethylene glycol, diethylene glycol and ethylene glycol in supercritical carbon dioxide up to 16 MPa at 313. 15 and 333. 15K. *Fluid Phase Equilibria* **52**, 365–372 (1989).
134. T. Yonemoto, T. Charoensombut-Amon, and R. Kobayashi, Triethylene glycol vaporization losses in supercritical CO2. *GPA Research Rep. Rep. No.* **RR-119**, 1–27 (1989).
135. F.-Y Jou., R.D. Deshmukh, F.D. Otto, and A.E. Mather, Vapor-liquid equilibria for acid gases and lower alkanes in triethylene glycol. *Fluid Phase Equilibria* **36**, 121–140 (1987).
136. M. Wise and A. Chapoy, Carbon dioxide solubility in triethylene glycol and aqueous solutions. *Fluid Phase Equilibria* **419**, 39–49 (2016).
137. D. Jerinic, J. Schmidt, K. Fischer, and L. Friedel, Measurement of the triethylene glycol solubility in supercritical methane at pressures up to 9 MPa. *Fluid Phase Equilibria* **264(1–2)**. 253–258 (2008).
138. L.C. Wilson, W.V. Wilding, and G.M. Wilson, Vapor–liquid equilibrium measurements on four binary mixtures. *AIChE Symp. Ser.* **85**(271), 25–43 (1989).

DOI: 10.7569/JNGE.2018.692501

139. R.L. Rowley and G.L. Hoffman, Vapor-liquid equilibrium measurements on mixtures important to industrial design: Triethylene glycol + n-hexane, triethylene glycol + cyclohexane, and furfural + isoprene. *AIChE Symp. Ser.* **86**(279), 6–19 (1990).
140. H.-J. Ng, C.-J. Chen, and D.B. Robinson, The influence of high concentrations of methanol on hydrate formation and the distribution of glycol in liquid-liquid mixtures. *GPA Midstream Association GPA* **RR-106**, (1987).
141. H.-J. Ng and D.B. Robinson, Hydrate formation in systems containing methane, ethane, propane, carbon dioxide or hydrogen sulfide in the presence of methanol. *Fluid Phase Equilibria*, **21**(1–2), 145–155 (1985).
142. M.J. Ross and L.S. Toczylkin, Hydrate dissociation pressures for methane or ethane in the presence of aqueous solutions of triethylene glycol. *J. Chem. Eng. Data* **37**(4), 488–491 (1992).
143. G.K. Folas, G.M. Kontogeorgis, M.L. Michelsen, and E.H. Stenby, Application of the cubic-plus-association equation of state to mixtures with polar chemicals and high pressures. *Ind. Eng. Chem. Res.* **45**(4), 1516–1526 (2006).
144. G.K. Folas, G.M. Kontogoorgis, M.L. Michelsen, and E.H. Stenby, Application of the cubic-plus-association equation of state to mixtures with polar chemicals and high pressures, *Ind. Eng. Chem. Res.* **45**(4), 1516–1526 (2006).
145. S.H. Huang and M. Radosz, Equation of state modeling for small, large, polydisperse and associating molecules. *Ind. Eng. Chem. Res.* ***29****(11)*, 2284–2294 (1990).
146. I. Tsivintzelis, G.M. Kontogeorgis, M.L. Michelsen, and E.H. Stenby, Modeling phase equilibria for acid gas mixtures using the CPA equation of state. Part II: Binary mixtures with CO2. *Fluid Phase Equilibria* **306**(1), 38–56 (2011).

DOI: 10.7569/JNGE.2018.692501

APPENDIX A

PR-CPA Model

The classical Peng-Robinson equation [12] with the volume correction as suggested by Peneloux et al. [14] takes the form

$$P = \frac{RT}{V-b}\frac{a(T)}{(V+c)(V+2c+b)(V-b)} \tag{A1}$$

For component i the a-parameter equals

$$a_i(T) = a_{ci}\alpha_i(T) \quad where \ \alpha_i(T) = \left(1 + m\left(1 - \sqrt{\frac{T}{T_{ei}}}\right)\right) \tag{A2}$$

The parameter a_{ci} is the a-parameter of component i at its critical temperature and evaluated from the critical temperature and pressure. The parameter m_i is determined from the acentric factor, ω_i. For the original PR-equation [12], the expression for m_i takes the form

$$m_i = 0.37464 + 1.54226\ \omega_i - 0.269922\omega_i^2 \tag{A3}$$

The PR modification from 1978 [13] uses the same expression for m_i for components with acentric factors not exceeding 0.49. For components with higher acentric factors, m_i is found from

$$m_i = 0.379642 + \omega_i(1.48503 - 0.164423\ \omega_i + 0.01666\omega_i^2) \tag{A4}$$

Mathias and Copeman [15] have suggested an alternative expression for $\alpha_i(T)$ of component i:

$$\alpha_i(T) = \left(1 + C_{1,i}\left(1 - \sqrt{\frac{T}{T_{ci}}}\right) + C_{2,i}\left(1 - \sqrt{\frac{T}{T_{ci}}}\right)^2 + C_{3,i}\left(1 - \sqrt{\frac{T}{T_{ci}}}\right)^3\right) for \sqrt{\frac{T}{T_{ci}}} < 1 \tag{A5}$$

$$\alpha_i(T) = \left(1 + C_{l,i}\left(1 - \sqrt{\frac{T}{T_{ei}}}\right)\right)^2 \quad for \sqrt{\frac{T}{T_{ci}}} > 1 \tag{A6}$$

$C_{1,i}$–$C_{3,i}$ are component specific constants. As the classical temperature dependence in Equation (A2) provides a good match of the vapor pressures of non-aqueous reservoir fluid constituents and the functional form of the Matias-Copeman expression reduces to the classical one for super-critical temperatures, it is seldom

DOI: 10.7569/JNGE.2018.692501

to see the Matias-Copeman expression used for water free petroleum reservoir fluids and the expression is not used in this work.

For mixtures, the equation of state parameters, a(T), b, and c are found from:

$$a(T) = \sum_i \sum_j x_i x_j \sqrt{a_i(T) a_j(T)} (1 - k_{ij}) \ \ where \ k_{ij} = k_{ij}^0 + k_{ij}(T - 288.15K) \tag{A7}$$

$$b = \sum_i x_i b_i \tag{A8}$$

$$c = \sum_i x_i c_i \quad where \ c_i = c_i^0 + c_i(T - 288.15K) \tag{A9}$$

x_i and x_j are mole fractions of components i and j and k_{ij} a binary interaction parameter for the same two components.

Vapor pressures and liquid densities of aqueous components are significantly higher than of hydrocarbon components of approximately the same molecular weight. The CPA theory attributes this to a fraction of the aqueous components associating with other molecules of the same species. The association term enters as a correction to the pressure from a classical cubic equation

$$P = P_{Cubic} + P_{Association} \tag{A10}$$

The association term used in this work takes the form [28]

$$P_{Association} = -\frac{1}{2}\frac{RT}{V}\left(1 - V\frac{\partial \ln g}{\partial V}\right)\sum_i^N \left(x_i \sum_{A_i}^{NS} \left(1 - X_{Ai}\right)\right) \tag{A11}$$

N is number of components and NS_i is the number of association sites (A_i) for component i. X_{A_i} is the fraction of molecules i not bonded at site A.

$$X_{Ai} = \frac{1}{1 + \frac{1}{V}\sum_{j=1}^{N}\sum_{B_j}^{NS} x_j X_{Bj} \Delta^{Ai,Bj}} \tag{A12}$$

where

$$\Delta^{Ai,Bj} = g(\eta)\left[\exp\left(\frac{\varepsilon^{A_i,B_j}}{RT}\right) - 1\right] b_{ij} \beta^{A_i B_j} \tag{A13}$$

$\varepsilon^{A_i B_j}$ and $\beta^{A_i B_j}$ are parameters expressing association energy and association volume for component pair i-j. NS_j is the number of association sites (B_j) for component j. X_{B_i} is the fraction of molecules j not bonded at site B. The parameter b_{ij}

DOI: 10.7569/JNGE.2018.692501

is the average of the b-parameters for components i and j. The radial distribution function used in this work is [5]

$$g(\eta) = \frac{1}{1-1.9\eta} \; where \; \eta = \frac{b}{4V} \tag{A14}$$

Two associating components of different species may cross-associate and evaluation of Equation (A12) requires a cross-association energy and a cross-association volume for each pair of cross-associating components. The combining rules of Voutsas et al. [16], often referred to as CR-1, are used in this work:

$$\varepsilon^{A_iB_j} = \frac{\varepsilon^{A_iB_j} + \varepsilon^{A_jB_i}}{2} \tag{A15}$$

$$\beta^{A_iB_j} = \sqrt{\beta^{A_iB_j}\beta^{A_jB_j}} \tag{A16}$$

CO_2 and H_2S do not self-associate ($\varepsilon^{A_iB_i}$ and $\beta^{A_iB_i}$ are zero), but may cross-associate with water. They are said to be solvating with water and hydrate inhibitors. For those two components, a modified CR-1 combining rule is used [16] and below exemplified for water:

$$\varepsilon^{A_iB_j} = \frac{\varepsilon^{A_iB_i} + \varepsilon^{A_{H_2O}B_{H_2O}}}{2} = \frac{\varepsilon^{A_{H_2O}B_{H_2O}}}{2} \tag{A17}$$

$$\beta^{A_iB_j} = \beta^{A_iB_{H_2O}} \tag{A18}$$

$\beta^{A_iB_{H_2O}}$ is a parameter specific for each solvating component and water. Similar parameters exist for the two solvating components and each hydrate inhibitor.

Non-aqueous components such as C_1 have no association sites, hence no values for neither self-association nor cross-association parameters. In turn, they do not contribute to the association term whether as pure components or as binaries with any other component.

An association scheme is required for each associating or solvating component. It tells the number of positive and negative association sites for each component. Table A1 shows the association schemes used in this work.

An association scheme represents a certain way of interaction between positive and negative sites of a component. Figure A1 illustrates the association schemes 4C with 2 positively charged and 2 negatively charged association sites and 2B with 1 positively charged and 1 negatively charged association site mentioned in Table A1. All positively charged sites can associate with all negatively charged sites and vice versa. Sites of same charge, positive or negative, cannot associate

DOI: 10.7569/JNGE.2018.692501

Table A1 Association schemes used in this work.

Component	No. of positive sites	No. of negative sites	Association scheme [20]
Water	2	2	4C
MeOH	1	1	2B
MEG	2	2	4C
TEG	2	2	4C
CO_2	0	1	-
H_2S	0	1	-

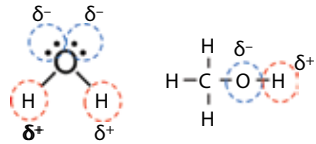

Figure A1 Illustration of association schemes 4C with 2 positively charged and 2 negatively charged association sites (left) and 2B with 1 positively charged and 1 negatively charged association site (right).

with each other. This gives 4 association sites for the 4C association scheme and 2 association sites for the 2B association scheme.

If a component self-associates, it affects the calculated critical point and the parameters a and b in the cubic term (Equation (A1)) cannot be determined from the critical temperature and pressure as is the case for a non-associating component. The parameters in the cubic term are instead determined from other property data. Volume correction is not used for associating components in this work, which means the c-parameter in Equation (A1) equals zero.

To make use of the PR-CPA model concept, five pure component parameters (a_0, b, c_1, ε^{AB}, and β^{AB}) must be determined for each associating component. The parameter a_0 is equivalent to a_c in Equation (A2), b is the b-parameter entering into the cubic term considering association, and c_1 is equivalent to m_i in Equation (A2). For a non-associating component, the association term is zero and there are no ε^{AB} and β^{AB} parameters. The sour gases, CO_2 and H_2S, are assumed to solvate with water. For those two inorganic gases the parameters in the cubic term can be determined as for other non-associating components, but to properly account for the interaction with water, a cross-association volume $\beta^{A_iB_{H_2O}}$ must be determined. The concept of solvation is described in [6] and successfully applied to similar systems elsewhere in the literature [29].

DOI: 10.7569/JNGE.2018.692501